

# Shell quenching in nuclear charge radii based on Monte Carlo dropout Bayesian neural network

Zhen-Yan Xian and Yan Ya

*School of Physics, Ningxia University, Yinchuan 750021, China*

Rong An\*

*School of Physics, Ningxia University, Yinchuan 750021, China*

*Guangxi Key Laboratory of Nuclear Physics and Technology,*

*Guangxi Normal University, Guilin, 541004, China and*

*Key Laboratory of Beam Technology of Ministry of Education,*

*College of Nuclear Science and Technology, Beijing Normal University, Beijing 100875, China*

Charge radii can be generally used to encode the information about various fine structures of finite nuclei. In this work, a constructed Bayesian neural network based on Monte Carlo dropout approach is proposed to accurately describe the charge radii of nuclei with proton number  $Z \geq 20$  and mass number  $A \geq 40$ . More motivated underlying mechanisms are incorporated into this combined model except for the basic building blocks with the specific proton and neutron numbers, which naturally contains the pairing effect, isospin effect, shell closure effect associated to the Casten factor  $P$ , valence neutrons, valence protons, quadrupole deformation  $\beta_{20}$ , high order hexadecapole deformation  $\beta_{40}$ , and the local “abnormal” shape staggering effect of  $^{181,183,185}\text{Hg}$ . To avoid the over-fitting puzzle along  $Z = 28, 50,$  and  $82$  isotopic chains, the modified Casten factor  $P^*$  is tentatively introduced into the input structure parameter sets. We have successfully demonstrated the ability of the Monte Carlo dropout Bayesian neural network (MC-dropout BNN) model to significantly increase the accuracy in predicting the nuclear charge radii. The standard root-mean-square deviation falls into  $0.0084$  fm for the training data and  $0.0124$  fm for the validation data with the modified Casten factor  $P^*$  input. Meanwhile, the shell closure effect of nuclear charge radii can be reproduced remarkably well.

## I. INTRODUCTION

Finite nuclei, which are characterized as the strongly correlated many-body systems, provide a natural probe to recognize the fundamental interactions and forces. As directly measured quantities in atomic nuclei, charge radii can be generally used to reflect the proton density distributions and encode the information about various fine structure phenomena, such as the emergence of shell closure effects [1–5] and the odd-even staggering (OES) behavior [6–9]. Furthermore, available description of pro-

ton density distributions can also be used to pin down the components of isospin interactions in the equation of state (EoS) of asymmetric nuclear matter [10–15]. This means that more data about nuclear charge radii should be urgently required with the highly accurate precision. Remarkable achievements have been obtained in detecting charge radii over the past decades. Especially for nuclei with extreme neutron-to-proton ratios, laser spectroscopy method can be considered as an available access to measure the nuclear size [16, 17].

The undertaken efforts have been devoted to featuring the normal and abnormal variations in nuclear charge radii along a long isotopic family, which includes

---

\* Corresponding author: [rongan@nxu.edu.cn](mailto:rongan@nxu.edu.cn)

the empirical formulas [18–21], relativistic mean field theory [22–24], non-relativistic Skyrme Hartree-Fock-Bogoliubov (HFB) approach [25, 26], and the Fayans energy density functional [27, 28], etc. Recently, machine learning methods have been made greatly applications in the course of nuclear physics [29–31]. Particularly, a well-known approach based on Bayesian neural network (BNN) has been widely and successfully employed to describe various nuclear quantities from finite nuclei to infinite nuclear matter, which includes the nuclear mass [32–41],  $\alpha$ -decay properties [42–45] and  $\alpha$ -clustering structure [46],  $\beta$ -decay properties [47–49] or double- $\beta$ -decay models [50–52],  $\gamma$ -ray emission [53], nuclear fission [54], low-lying excited phenomena [55, 56], landscape of nuclide chart [57, 58], neutron skin thickness [59, 60], the yields of production cross sections [61–63], and nuclear charge radii [64–68], etc. Besides, the Bayesian inference has a guidance to gain deeper insights into the understanding of fundamental interactions [69–76], significantly the bulk properties of nuclear matter [77–92]. It should be mentioned that Bayesian neural networks can cover the quantitative uncertainties associated with these various physical systems [93–107]. This encourages us to perform the proceeding researches in exploring the systematical evolution of nuclear charge radii through Bayesian neural network based approach.

Accurate description of nuclear charge radii can be applied to refine the local variations in nuclear size. In Ref. [64], it demonstrates that the BNN can increase the prediction ability of nuclear charge radii by training the residuals between the theoretical predictions and experimental data. This leads to the root-mean-square (rms) deviation with being around 0.02 fm. The improved BNN which considers the pairing and shell closure effects gives the rms deviation 0.015 fm in calibrating the charge radii data of nuclei with mass number  $A \geq 40$  and proton number  $Z \geq 20$  [67]. As is well known, the larger odd-even staggering in charge radii can be profoundly observed in the neutron-deficient isotopes around the proton number

$Z = 82$  isotopic chains [7, 9, 108–111]. This is attributed to the underlying mechanism of the abrupt shape-phase transition. By considering the abnormal shape staggering effect, the standard rms deviation falls into 0.014 fm for both the trained and validated charge radii data through the refined Bayesian neural network [68]. In addition, different kinds of machine learning methods, such as the naive Bayesian probability classifier [65] and artificial neural networks [66, 112, 113], can be used to explore the systematical evolution of nuclear charge radii as well.

As mentioned above, the Bayesian neural networks can capture the considered error quantification through comparing the experimental data and theoretical simulations. Moreover, this probabilistic model is more computational saving with respect to the generally used energy density functionals (EDFs). As mentioned in Ref. [114], the aleatoric and epistemic uncertainties should be explicitly considered in a given Bayesian neural network. This means that more complex input structures should be taken into account in the simulating process. In other words, more underlying physical mechanisms should be captured as much as possible in the calibrated protocol. To further reduce the quantified uncertainty in validating the nuclear charge radii, both of the quadrupole deformation  $\beta_{20}$  and higher moment deformation  $\beta_{40}$  are incorporated into the training process in this work. The Casten factor  $P$ , which is characterized as the correlation between the valence neutrons  $\nu_n$  and the valence protons  $\nu_p$ , is associated to the shell closure effect [115–117]. In our calculations, the Casten factor  $P$ , valence neutrons  $\nu_n$ , and valence protons  $\nu_p$  are simultaneously considered as the input parameter sets.

Actually, Casten factor  $P$  plays an indispensable role in the calibrated protocol [67, 68, 118]. For the calculation of the Casten factor  $P$ , the reference neutron and proton magic numbers are taken as  $Z = 2, 6, 14, 28, 50, 82, (114)$  and  $N = 2, 8, 14, 28, 50, 82, 126, (184)$  [10, 116, 118]. However, the traditional Casten factor, which is defined as  $P = \nu_n \nu_p / (\nu_n + \nu_p)$  is invalid along  $Z = 28, 50, 82$  iso-

topic chains due to the fully filled proton magic shells. In order to avoid the aforementioned problem, the shell closure effect has been taken into account through the modified Casten factor  $P^*$ . In this work, the Monte Carlo dropout Bayesian neural network (MC-dropout BNN) approach is built appropriately to describe the charge radii of nuclei with proton number  $Z \geq 20$  and mass number  $A \geq 40$ . The input structures include the proton number ( $Z$ ), mass number ( $A$ ), the pairing effect ( $\delta$ ), isospin effect ( $I^2$ ), shell closure effect associated to the Casten factor  $P^*$ , valence neutrons  $\nu_n$ , valence protons  $\nu_p$ , quadrupole deformation  $\beta_{20}$ , high order hexadecapole deformation  $\beta_{40}$ , and the local ‘‘abnormal’’ shape staggering effect of  $^{181,183,185}\text{Hg}$  ( $LI$ ). The results obtained by incorporating the traditional Casten factor  $P$  into the input structures are also shown for comparison.

The structure of the paper is the following. In Sec. II, the theoretical framework about the MC-dropout BNN approach is briefly presented, which includes the engineered features and the training and validation data sets in the nuclear charge radii. In Sec. III, the numerical results and discussion are provided. Finally, a summary is given in Sec. IV.

## II. THEORETICAL FORMALISM

The Bayesian neural network (BNN), which is characterized as the combination of an artificial neural network (ANN) and the Bayesian statistical theory, provides a potential approach to comprehend the physical quantities with the associated uncertainty. However, as demonstrated in Ref. [119], the over-fitting puzzle can be encountered in the traditional neural network. Then the proposed dropout approach can be used to avoid over-fitting problem of the neural network parameters through the regularization technique. Meanwhile, the constructed Monte Carlo dropout (MC-dropout) method is being equivalent to variational inference Bayesian learning method in evaluating a neu-

ral network [120]. Therefore the Monte Carlo dropout Bayesian neural network (MC-dropout BNN) model has been built based on these motivations. This approach has been successfully used to analyze various physical quantities, such as the spectral function [121], mass distributions of the induced fission [122], and electron-carbon scattering data [123].

The dropout architecture with a single hidden layer can be recalled as follows,

$$\hat{y} = \sigma(xz_1W_1 + b)z_2W_2, \quad (1)$$

where  $\sigma$  depicts the nonlinear activation function,  $x$  represents the input data,  $W_1$  represents the weight matrix connecting the input layer to the hidden layer,  $b$  denotes the bias vectors, and  $W_2$  represents the weight matrix that links the hidden to output layer.  $z_1$  and  $z_2$  are binary vectors in the sampling process. MC-dropout approach is driven by the Bernoulli distributed random variables in the multiplying hidden activations. The random variables take the value of 1 with probability parameter  $p$  and 0 for other cases [120]. This means the neuron is invalid if the corresponding binary variable takes 0 in a given input.

The  $L_2$  regularization weighted by some weight decay gives a minimization objective shown as follows [122, 124],

$$L_{\text{dropout}} = \frac{1}{N} \sum_{n=1}^N \|y_n - \hat{y}_n\|_2^2 + \lambda_{\text{decay}} \sum_{i=1}^L (\|W_i\|_2^2 + \|b_i\|_2^2). \quad (2)$$

The first term denotes the Euclidean loss function used in the training and optimization process of neural network. Where  $\hat{y}_n$  represents the output of a neural network with  $L$  layers and  $y_n$  denotes the target value.  $N$  is the number of training data points. A regularization term is often added into the optimization process as shown in the second term. Here, the weight matrixes of dimensions  $K_i \times K_{i-1}$  are represented by  $W_i$  and the bias vectors of dimensions  $K_i$  for each layer  $i = 1, 2, \dots, L$  are denoted

by  $b_i$ . The quantity  $\lambda_{\text{decay}}$  represents the regularization parameter [122].

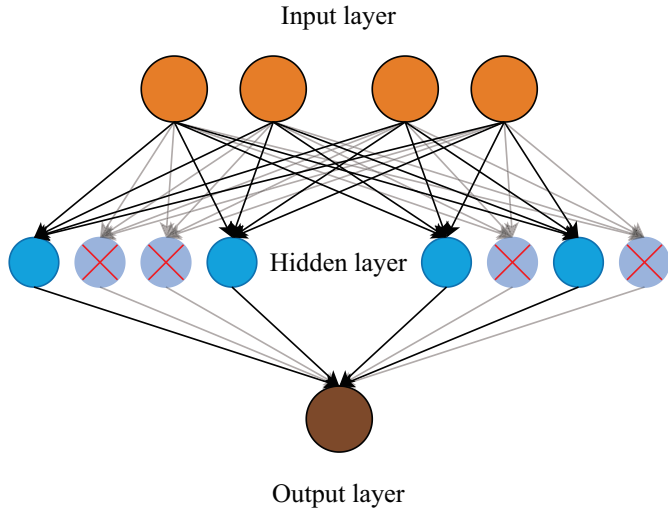


FIG. 1. (Color online) Structure of the Monte Carlo dropout Bayesian neural network used in this work. The number of neurons in the input layer is 10. The 3 hidden layers are employed, and the number of neurons in the corresponding hidden layer 1 and 3 are 28 and 71, respectively. The hidden layer 2, namely the dropout layer, has 300 neurons. This diagrammatic sketch just shows the dropout hidden layer, in which the different markers denote the random variables take value of 1 with probability parameter  $p$  and 0 for other cases. The number of neurons in the output layer is 1.

Shown in Refs. [114, 125], the predicted errors of the observables are mainly originated from epistemic uncertainty and aleatoric uncertainty in using machine learning approaches. This means the chosen input structure parameter sets should capture the underlying physical mechanisms as much as possible. In this work, the experimental charge radii data of nuclei with  $Z \geq 20$  and  $A \geq 40$  are used to train the MC-dropout BNN [111, 126, 127]. As mentioned in *Introduction*, the input structures for the MC-dropout BNN are consisted of the proton number ( $Z$ ), mass number ( $A$ ), isospin asymmetry degree ( $I^2$ ), pairing effect ( $\delta$ ), Casten factor ( $P$ ), valence neutrons ( $\nu_n$ ) and protons ( $\nu_p$ ), quadrupole deformation ( $\beta_{20}$ ), the hexadecapole deformation ( $\beta_{40}$ ), and the profound shape-phase transition in  $^{181,183,185}\text{Hg}$  ( $LI$ ). The ground state properties about quadrupole and hexadecapole deformation parameters are taken from Ref. [128].

The final input structures for the MC-dropout BNN approach are  $z = \{Z, A, I^2, \delta, P, \nu_n, \nu_p, \beta_{20}, \beta_{40}, LI\}$ , in which

$$I^2 = \left(\frac{N-Z}{A}\right)^2, \quad (3)$$

$$\delta = \frac{(-1)^Z + (-1)^N}{2}, \quad (4)$$

$$P = \frac{\nu_p \nu_n}{\nu_p + \nu_n}, \quad (5)$$

$$LI = \begin{cases} 1, & (Z, A) = (80, 181), (80, 183), (80, 185) \\ 0, & \text{else} \end{cases} \quad (6)$$

As mentioned before, the traditional Casten factor  $P$  is invalid along the proton magic numbers  $Z = 28, 50, 82$  isotopic chains. To avoid this puzzle, the modified Casten factor  $P^*$  is proposed as follows,

$$P^* = \ln \left( \frac{e^{\nu_p} e^{\nu_n}}{\nu_p + \nu_n} \right). \quad (7)$$

The input parameter sets which includes the traditional Casten factor  $P$  cannot describe the shell quenching phenomena around the neutron magic numbers. In contrast to the traditional Casten factor  $P$ , the modified Casten factor  $P^*$  can give more high accuracy in the training and validation sets, and the shell closure effect in charge radii can be reproduced well. More details can be found in the following *Section*. For the modified Casten factor  $P^*$ , the input structures can be redefined as  $z = \{Z, A, I^2, \delta, P^*, \nu_n, \nu_p, \beta_{20}, \beta_{40}, LI\}$ . Meanwhile, if the proton numbers and neutron numbers simultaneously occupy the fully filled shells, such as  $(Z = 28, N = 28)$ ,  $(Z = 28, N = 50)$ ,  $(Z = 50, N = 50)$ ,  $(Z = 50, N = 82)$ , and  $(Z = 82, N = 126)$  cases, two kinds of Casten factors are vanished totally. In addition, the np formula [129] can also be chosen as our theoretical model to be refined by MC-dropout BNN:

$$R_{\text{np}}(Z, A) = r_0 A^{1/3} \left( 1 - b \frac{N-Z}{A} + \frac{c}{A} \right), \quad (8)$$

where  $r_0 = 0.966$  fm,  $b = 0.182$ , and  $c = 1.652$  [130].

### III. RESULTS AND DISCUSSION

For the convenience of discussion, we use “ $P^*$ ” to denote the model combining NP formula and the MC-dropout BNN with input neurons  $z = \{Z, A, I^2, \delta, P^*, \nu_n, \nu_p, \beta_{20}, \beta_{40}, LI\}$ . We also give the results obtained by the MC-dropout BNN with input neurons  $z = \{Z, A, I^2, \delta, P, \nu_n, \nu_p, \beta_{20}, \beta_{40}, LI\}$ , denoted by “ $P$ ” for comparison. Here, we should be mentioned that the difference between  $P^*$  and  $P$  just distinguishes the local variations in charge radii along  $Z = 28, 50, 82$  isotopic families. In the training set, we use the 815 experimental data given in Ref. [126]. The more recent experimental data [111, 127], containing 118 data for nuclei with  $Z \geq 20$  and  $A \geq 40$ , are used as the validation set to test the predictive power of our model. In contrast to Refs. [67, 68], the training data sets are reduced owing to the whole data of charge radii along nickel isotopic chain are transformed into the validation data set.

To further quantify the predictive power, the rms deviation between the results obtained by the MC-dropout BNN model and the corresponding experimental data are calculated as follows,

$$\sigma^{(T,V,TV)} = \sqrt{\frac{1}{N_{(T,V,TV)}} \sum_{i=1}^{N_{(T,V,TV)}} \left( R_{\text{ch},i}^{\text{pred.}} - R_{\text{ch},i}^{\text{exp.}} \right)^2}. \quad (9)$$

where  $N_T$ ,  $N_V$ , and  $N_{TV}$  are the numbers of charge radii contained in the training (T), validation (V), and entire (TV) data sets, and the subscript  $i$  represents the  $i$ th nucleus in the given data sets.

As shown in Ref. [67], the predictive accuracy in describing the rms charge radii has been achieved to be  $\sigma^T = 0.0143$  fm, and  $\sigma^{TV} = 0.0149$  fm. Then the revised version has been proposed to further reduce the quantitative uncertainty [68], which leads to the  $\sigma^T = 0.0140$  fm and  $\sigma^{TV} = 0.0139$  fm. For these studies, the Casten factor associated to the valence neutrons and protons is regarded as input parameter. However, the quadrupole deformation has not been taken into account in the val-

idated protocol. As demonstrated in Ref. [10], the rms deviation in charge radii can be reduced if the shape deformation is incorporated into the calibrated protocol. In recent study, the input sets  $\{Z, A, \delta, \nu_p, \nu_n, \beta_{20}\}$  have been used in the training and validation data set, the rms deviation has been fallen into  $\sigma^T = 0.0106$  fm and  $\sigma^{TV} = 0.0130$  fm [114].

TABLE I. Root-mean-square (rms) deviations of charge radii predicted by the  $P$  and  $P^*$  models.

Model	$\sigma^{(T)}$	$\sigma^{(V)}$	$\sigma^{(TV)}$
P	0.0124 fm	0.0147 fm	0.0128 fm
$P^*$	0.0084 fm	0.0124 fm	0.0092 fm

In Table I, the  $\sigma^T$ ,  $\sigma^V$ , and  $\sigma^{TV}$  values derived from the Eq. (9) are shown, respectively. In our calculations, the valence neutrons, valence protons, Casten factor, and the shape-phase deformation in the limited region are simultaneously taken into account during the simulated process. Meanwhile, the higher deformation parameter  $\beta_{40}$  is also included. The deduced value of  $\sigma^{TV}$  deriving from the  $P$  model is equivalent to Ref. [114], but less than the results shown in Refs. [67, 68]. As mentioned above, the over-fitting puzzle can be encountered in the traditional Casten factor  $P$  when meets the isotopic chains with proton numbers  $Z = 28, 50, 82$ . The  $\sigma^{TV}$  value obtained by  $P^*$  model can be further reduced to be 0.0094 fm. This is accord with Ref. [68] where the modified rms deviation has been used to measure the quantified uncertainty. In a word, the rms deviations in the training and validation data sets are also further reduced with respect to those investigations in the existing literature. It is therefore reasonable to demonstrate the predictive power of the  $P^*$  model by modifying the traditional Casten factor  $P$ . Significant improvement has been achieved by the  $P^*$  model in both the interpolation and the extrapolation predictions of nuclear charge radii in comparison with the  $P$  model. To visualize the details about the training and validation of the MC-dropout BNN approach, as shown in Fig. 2, the difference between the calibrated rms charge radii with  $P^*$  model and the corresponding

experimental data are depicted in nuclear chart. From this figure, it can be found that most of the experimental data can be reproduced well. In some specific regions, the predicted values are heavily deviated from the experimental data. As is well known, the inverse OES or the weakened OES can be evidently observed around Eu ( $Z = 63$ ) [131] and At ( $Z = 85$ ) [132] isotopes. In our calibrated protocol, the inverse odd-even staggering behavior has not been considered properly. This seems to lead the larger deviations between the predicted rms charge radii and the corresponding experimental data. Meanwhile, the larger deviations can also be encountered along manganese isotopes. This means that more underlying mechanisms should be covered through the input structures.

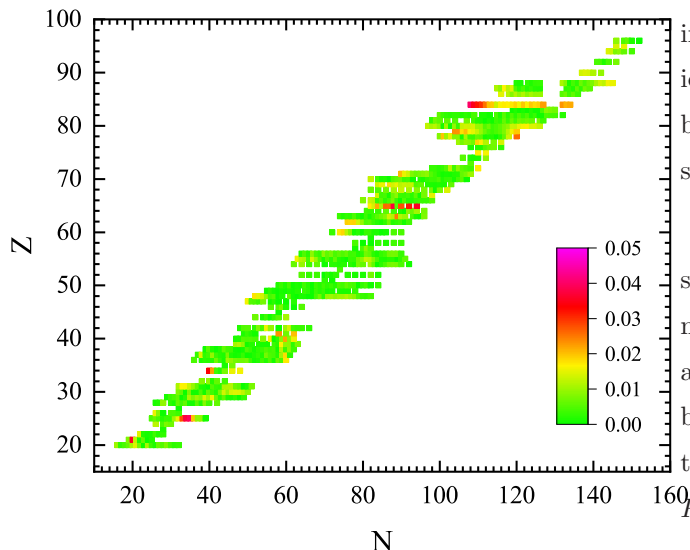


FIG. 2. (Color online) Nuclear chart displaying the absolute differences (in units of fm) between the MC-Dropout BNN predicted rms charge radii and the experimental data in the entire set. The results are obtained from the training and validation procedures, respectively.

Shell closure effects are naturally observed in charge radii throughout the whole nuclear chart [126, 127, 133–135]. This attributes to the rather small isospin dependence of the spin-orbit interactions [136]. The relativistic mean field theory [22–24] and the Fayans energy density

functional model [27, 28] can reproduce the shell quenching phenomena in nuclear charge radii well. However, as demonstrated in Ref. [133], the Skyrme density functional theory cannot reproduce the shell closure effects. This provides an potential signature to identify the predictive power of nuclear models in describing the local variations of charge radii. In Fig. 3, the rms charge radii of calcium (a), nickel (b), tin (c), and lead (d) isotopes are depicted with both of the  $P^*$  and  $P$  models, respectively. As mentioned above, MC-dropout BNN model can provide the quantified uncertainty in the validated process. Therefore the corresponding error bars are also shown in Fig. 3. For calcium isotopes,  $P^*$  and  $P$  models give the similar trend of changes of charge radii. The slight deviations can be found at the neutron-deficient  $^{34}\text{Ca}$  and neutron-rich  $^{54,55}\text{Ca}$  isotopes. Meanwhile, charge radii of  $^{39,43}\text{Ca}$  isotopes can be reproduced well by the  $P^*$  model

in comparing with the  $P$  model. Likewise, the systematical evolution of charge radii along tin isotopes can also be reproduced well by both of the  $P^*$  and  $P$  models as shown in Fig. 3 (c).

In Fig. 3 (b), it is obviously found that the  $N = 28$  shell closure effect cannot be reproduced well by the  $P$  model. Besides, the charge radii of  $^{54-56,58}\text{Ni}$  isotopes are heavily overestimated. The same scenarios can also be found in the  $^{65-68}\text{Ni}$  isotopes, but with slight deviation. Meanwhile, charge radius of  $^{70}\text{Ni}$  obtained by the  $P$  model is slightly underestimated with respect to  $P^*$  model. Toward proton-rich regions, the pronounced deviations can be obviously exhibited between the predictive results obtained by the  $P^*$  and  $P$  models. These larger deviations can also be encountered in the neutron-rich lead isotopes as shown in Fig. 3 (d). Here, it should be mentioned that the rapid increase of charge radii can be reproduced well by the  $P^*$  model, but the  $P$  model fails to follow this trend beyond the neutron number  $N = 126$ . All of these results suggest that  $P^*$  model can provide a powerful prediction of nuclear charge radii. Therefore, the extrapolated simulation with high accuracy is nec-

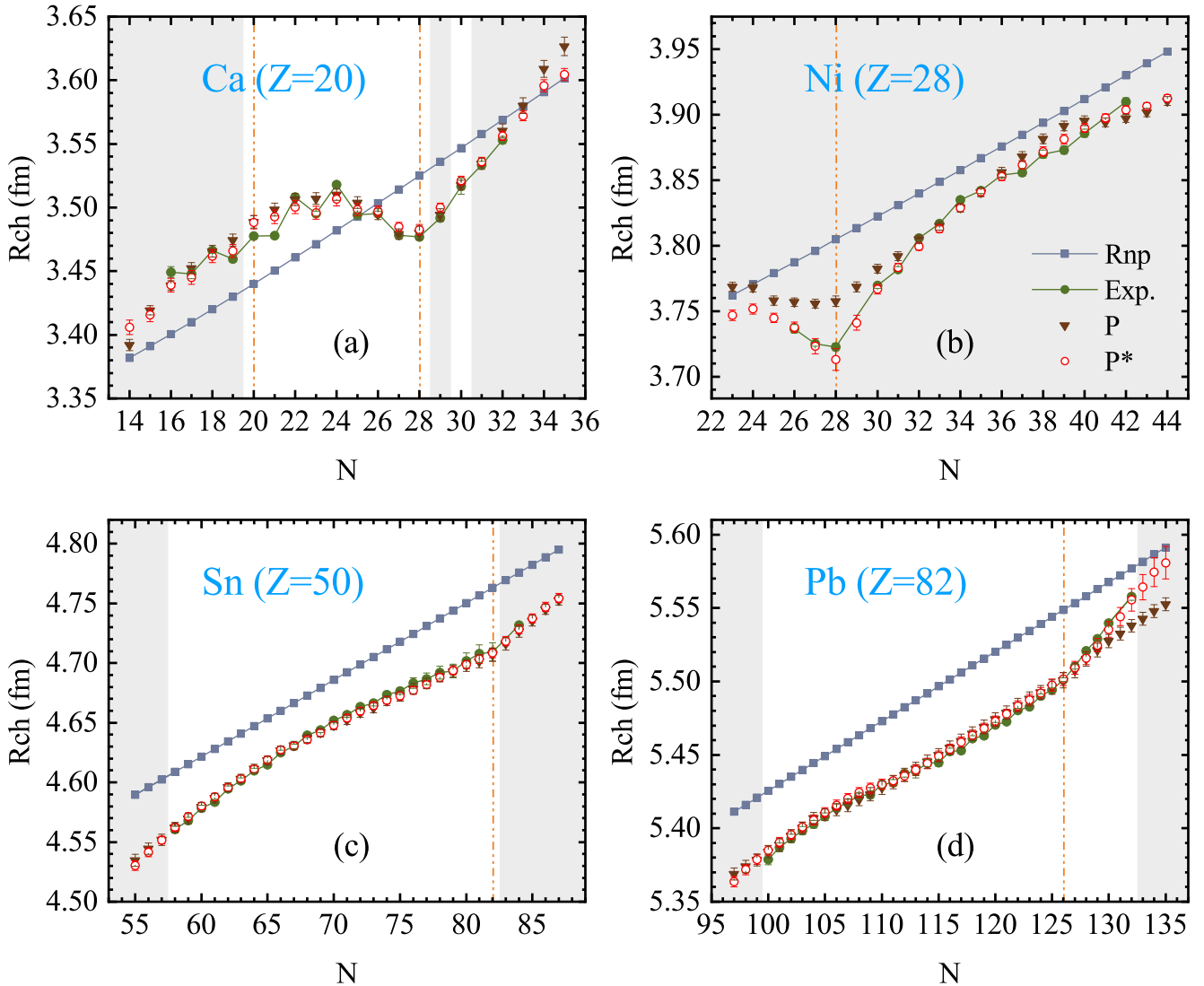


FIG. 3. (Color online) Root-mean-square charge radii of calcium (a), nickel (b), tin (c), and lead (d) isotopes simulated by the  $P^*$  and  $P$  models, in comparison with the experimental data [126, 127]. The results obtained by the np formula ( $R_{np}$ ) are also drawn for making a guide eye. The data covered by gray area are not contained in the training set, namely the pure predictions. The neutron magic numbers  $N = 20, 28, 50, 82$ , and 126 are emphasized by the vertical lines.

essary. In Table II, charge radii of calcium, nickel, tin, and lead isotopes are shown explicitly. These results are encouraged to provide an theoretical guidance for the experimental researches.

The input parameters which include the modified Casten factor  $P^*$  can describe the systematical evolution of nuclear charge radii well. This can be easily found from the rms deviation of the training and validation data sets. Furthermore, as shown in Fig. 3, the shrunk phenomena in charge radii can be reproduced well with the  $P^*$

model. Actually, Casten factor represents the neutron-proton correlation in describing the trend of changes of nuclear charge radii. As demonstrated in Refs. [137–139], the neutron-proton correlation has an influence on determining the nuclear charge radii. This can also be found from Refs. [23, 24] where the neutron-proton correlation derived from the difference of the fractions of Cooper pairs between neutrons and protons can reproduce the shell quenching in charge radii as well. All of these suggest that more appropriate isospin interactions should be

TABLE II. The root-mean-square charge radii predicted by the  $P^*$  and  $P$  models, respectively.

Nucleus	$P^*$ model	$P$ model
$^{34}\text{Ca}$	3.4059(56)	3.3920(44)
$^{35}\text{Ca}$	3.4156(53)	3.4193(37)
$^{53}\text{Ca}$	3.5721(40)	3.5800(62)
$^{54}\text{Ca}$	3.5956(48)	3.6089(65)
$^{55}\text{Ca}$	3.6046(47)	3.6267(72)
$^{51}\text{Ni}$	3.7470(40)	3.7687(33)
$^{52}\text{Ni}$	3.7517(40)	3.7682(35)
$^{53}\text{Ni}$	3.7448(35)	3.7581(35)
$^{57}\text{Ni}$	3.7412(56)	3.7686(38)
$^{69}\text{Ni}$	3.8976(32)	3.8942(36)
$^{71}\text{Ni}$	3.9066(28)	3.9019(32)
$^{72}\text{Ni}$	3.9128(27)	3.9105(33)
$^{105}\text{Sn}$	4.5303(40)	4.5348(51)
$^{106}\text{Sn}$	4.5414(36)	4.5446(47)
$^{107}\text{Sn}$	4.5517(33)	4.5519(46)
$^{133}\text{Sn}$	4.7183(38)	4.7162(52)
$^{135}\text{Sn}$	4.7375(36)	4.7355(45)
$^{136}\text{Sn}$	4.7471(39)	4.7450(42)
$^{137}\text{Sn}$	4.7545(40)	4.7527(42)
$^{179}\text{Pb}$	5.3638(35)	5.3688(41)
$^{180}\text{Pb}$	5.3718(34)	5.3740(42)
$^{181}\text{Pb}$	5.3787(33)	5.3785(42)
$^{213}\text{Pb}$	5.5441(62)	5.5326(44)
$^{215}\text{Pb}$	5.5642(85)	5.5426(44)
$^{216}\text{Pb}$	5.5744(99)	5.5479(44)
$^{217}\text{Pb}$	5.5808(111)	5.5525(44)

covered in describing the nuclear charge radii. Especially, the difference of charge radii can be used to ascertain the nuclear symmetry energy through the mirror-pair nuclei. Thus more available charge radii data are required in theoretical study.

#### IV. SUMMARY AND CONCLUSIONS

More input parameter sets physically motivated, such as proton number, mass number, isospin-asymmetry degree, pairing effect, shell closure effect, valence neutrons and protons, Casten factor  $P$  or  $P^*$ , local shape-staggering phenomena, quadrupole deformation  $\beta_{20}$ , and

higher order  $\beta_{40}$  deformation, have been taken into account in the evaluated process. Significant improvements can be achieved in training and validating data sets. Especially, based on the  $P^*$  model, the rms deviations for the training and validation stage fall into  $\sigma^T = 0.0084$  fm and  $\sigma^V = 0.0124$  fm, and  $\sigma^{TV} = 0.0092$  fm for entire set.  $P^*$  model can reproduce the shell quenching phenomena and the rapid increase of charge radii across neutron magic numbers. This suggests that  $P^*$  model persists the predictive power when the theoretical uncertainties are taken into account. Even for nuclei located far from those contained in the training set,  $P^*$  model can still make available predictions.

This work presents the potential approach of Bayesian neural network in exploring nuclear charge radii. We should mention that physically motivated features play an indispensable role in extrapolating cases far away from the  $\beta$ -stability line. Although the Monte Carlo dropout Bayesian neural network provides rather small root-mean-square deviation in simulating the theoretical results, the larger deviation can also be encountered in some local regions. This means the underlying physical mechanism cannot be captured adequately in the training and validation data sets. In addition, the number of training data sets has an influence on describing and predicting the nuclear charge radii. Therefore, more complex input structures should be taken into account properly in the proceeding research.

#### ACKNOWLEDGEMENTS

This work was supported by the Open Project of Guangxi Key Laboratory of Nuclear Physics and Nuclear Technology, No. NLK2023-05 and the Central Government Guidance Funds for Local Scientific and Technological Development, China (No. Guike ZY22096024).

---

[1] I. Angeli and K. P. Marinova, J. Phys. G 42 (2015) 055108.

<https://dx.doi.org/10.1088/0954-3899/42/5/055108>



- [2] H. Nakada, *Phys. Rev. C* 100 (2019) 044310. <https://link.aps.org/doi/10.1103/PhysRevC.100.044310>
- [3] R. Garcia Ruiz and A. Vernon, *Eur. Phys. J. A* 56 (2020) 136. <https://doi.org/10.1140/epja/s10050-020-00134-8>
- [4] U. C. Perera, A. V. Afanasjev, and P. Ring, *Phys. Rev. C* 104 (2021) 064313. <https://link.aps.org/doi/10.1103/PhysRevC.104.064313>
- [5] S. Kaur, R. Kanungo, W. Horiuchi, G. Hagen, J. D. Holt, B. S. Hu, et al., *Phys. Rev. Lett.* 129 (2022) 142502. <https://link.aps.org/doi/10.1103/PhysRevLett.129.142502>
- [6] R. F. Garcia Ruiz, M. L. Bissell, K. Blaum, A. Ekstrom, N. Frommgen, G. Hagen, et al., *Nature Phys.* 12 (2016) 594, arXiv:1602.07906 [nucl-ex]. <https://doi.org/10.1038/nphys3645>
- [7] B. A. Marsh, T. Day Goodacre, S. Sels, Y. Tsunoda, B. Andel, A. N. Andreyev, et al., *Nature Phys.* 14 (2018) 1163. <https://doi.org/10.1038/s41567-018-0292-8>
- [8] A. J. Miller, K. Minamisono, A. Klose, D. Garand, C. Kujawa, J. D. Lantis, et al., *Nature Phys.* 15 (2019) 432. <https://www.nature.com/articles/s41567-019-0416-9>
- [9] A. Barzakh, A. N. Andreyev, C. Raison, J. G. Cubiss, P. Van Duppen, S. Péru, et al., *Phys. Rev. Lett.* 127 (2021) 192501. <https://link.aps.org/doi/10.1103/PhysRevLett.127.192501>
- [10] N. Wang and T. Li, *Phys. Rev. C* 88 (2013) 011301(R). <https://link.aps.org/doi/10.1103/PhysRevC.88.011301>
- [11] B. A. Brown, *Phys. Rev. Lett.* 119 (2017) 122502. <https://link.aps.org/doi/10.1103/PhysRevLett.119.122502>
- [12] B. A. Brown, K. Minamisono, J. Piekarewicz, H. Hergert, D. Garand, A. Klose, et al., *Phys. Rev. Res.* 2 (2020) 022035. <https://link.aps.org/doi/10.1103/PhysRevResearch.2.022035>
- [13] S. V. Pineda, K. K?nig, D. M. Rossi, B. A. Brown, A. Incorvati, J. Lantis, et al., *Phys. Rev. Lett.* 127 (2021) 182503. <https://link.aps.org/doi/10.1103/PhysRevLett.127.182503>
- [14] R. An, S. Sun, L.-G. Cao, and F.-S. Zhang, *Nucl. Sci. Tech.* 34 (2023) 119. <https://doi.org/10.1007/s41365-023-01269-1>
- [15] K. K?nig, J. C. Berengut, A. Borschevsky, A. Brinson, B. A. Brown, A. Dockery, et al., *Phys. Rev. Lett.* 132 (2024) 162502. [erratum: *Phys. Rev. Lett.* 133 (2024) 059901.] <https://link.aps.org/doi/10.1103/PhysRevLett.132.162502>
- [16] P. Campbell, I. Moore, and M. Pearson, *Prog. Part. Nucl. Phys.* 86 (2016) 127. <https://www.sciencedirect.com/science/article/pii/S01466410150009>
- [17] X. Yang, S. Wang, S. Wilkins, and R. G. Ruiz, *Prog. Part. Nucl. Phys.* 129 (2023) 104005. <https://www.sciencedirect.com/science/article/pii/S01466410220009>
- [18] S. Q. Zhang, J. Meng, S. G. Zhou, and J. Y. Zeng, *Eur. Phys. J. A* 13 (2002) 285. <https://doi.org/10.1007/s10050-002-8757-6>
- [19] D. Ni, Z. Ren, T. Dong, and Y. Qian, *Phys. Rev. C* 87 (2013) 024310. <https://link.aps.org/doi/10.1103/PhysRevC.87.024310>
- [20] J. Piekarewicz, M. Centelles, X. Roca-Maza, and X. Viñas, *Eur. Phys. J. A* 46, 379 (2010). <https://doi.org/10.1140/epja/i2010-11051-8>
- [21] M. Bao, Y. Lu, Y. M. Zhao, and A. Arima, *Phys. Rev. C* 94 (2016) 064315. <https://link.aps.org/doi/10.1103/PhysRevC.94.064315>
- [22] L.-S. Geng, H. Toki, S. Sugimoto, and J. Meng, *Prog. Theor. Phys.* 110 (2003) 921. <https://doi.org/10.1143/PTP.110.921>
- [23] R. An, L.-S. Geng, and S.-S. Zhang, *Phys. Rev. C* 102 (2020) 024307. <https://link.aps.org/doi/10.1103/PhysRevC.102.024307>
- [24] R. An, X. Jiang, N. Tang, L.-G. Cao, and F.-S. Zhang, *Phys. Rev. C* 109 (2024) 064302. <https://link.aps.org/doi/10.1103/PhysRevC.109.064302>
- [25] S. Goriely, S. Hilaire, M. Girod, and S. Péru, *Phys. Rev. Lett.* 102 (2009) 242501. <https://link.aps.org/doi/10.1103/PhysRevLett.102.242501>
- [26] S. Goriely, N. Chamel, and J. M. Pearson, *Phys. Rev. C* 82 (2010) 035804. <https://link.aps.org/doi/10.1103/PhysRevC.82.035804>
- [27] P.-G. Reinhard and W. Nazarewicz, *Phys. Rev. C* 95 (2017) 064328. <https://link.aps.org/doi/10.1103/PhysRevC.95.064328>
- [28] C. Gorges, L. V. Rodríguez, D. L. Balabanski, M. L. Bissell, K. Blaum, B. Cheal, et al., *Phys. Rev. Lett.* 122 (2019) 192502. <https://link.aps.org/doi/10.1103/PhysRevLett.122.192502>

- [29] L. Neufcourt, Y. Cao, W. Nazarewicz, and F. Viens, *Phys. Rev. C* 98 (2018) 034318. <https://link.aps.org/doi/10.1103/PhysRevC.98.034318>
- [30] P. Bedaque, A. Boehnlein, M. Cromaz, M. Diefenthaler, L. Elouadrhiri, T. Horn, et al., *Eur. Phys. J. A* 57 (2021) 100. <https://doi.org/10.1140/epja/s10050-020-00290-x>
- [31] J.-F. Paquet, *J. Phys. G* 51 (2024) 103001. <https://dx.doi.org/10.1088/1361-6471/ad6a2b>
- [32] R. Utama, J. Piekarewicz, and H. B. Prosper, *Phys. Rev. C* 93 (2016) 014311. <https://link.aps.org/doi/10.1103/PhysRevC.93.014311>
- [33] R. Utama and J. Piekarewicz, *Phys. Rev. C* 96 (2017) 044308. <https://link.aps.org/doi/10.1103/PhysRevC.96.044308>
- [34] Z. M. Niu and H. Z. Liang, *Phys. Lett. B* 778 (2018) 48. <https://doi.org/10.1016/j.physletb.2018.01.002>
- [35] Z. M. Niu, J. Y. Fang, and Y. F. Niu, *Phys. Rev. C* 100 (2019) 054311. <https://link.aps.org/doi/10.1103/PhysRevC.100.054311>
- [36] V. Kejzlar, L. Neufcourt, W. Nazarewicz, and P.-G. Reinhard, *J Phys. G* 47 (2020) 094001. <https://dx.doi.org/10.1088/1361-6471/ab907c>
- [37] X. H. Wu and P. W. Zhao, *Phys. Rev. C* 101 (2020) 051301. <https://link.aps.org/doi/10.1103/PhysRevC.101.051301>
- [38] Y. Liu, C. Su, J. Liu, P. Danielewicz, C. Xu, and Z. Ren, *Phys. Rev. C* 104 (2021) 014315. <https://link.aps.org/doi/10.1103/PhysRevC.104.014315>
- [39] A. E. Lovell, A. T. Mohan, T. M. Sprouse, and M. R. Mumpower, *Phys. Rev. C* 106 (2022) 014305. <https://link.aps.org/doi/10.1103/PhysRevC.106.014305>
- [40] Z. M. Niu and H. Z. Liang, *Phys. Rev. C* 106 (2022) L021303. <https://link.aps.org/doi/10.1103/PhysRevC.106.L021303>
- [41] X. Zhang, W. Li, J. Fang, and Z. Niu, *Nucl. Phys. A* 1043 (2024) 122820. <https://doi.org/10.1016/j.nuclphysa.2024.122820>
- [42] U. B. Rodríguez, C. Z. Vargas, M. Gonçalves, S. B. Duarte, and F. Guzmán, *J Phys. G* 46 (2019) 115109. <https://dx.doi.org/10.1088/1361-6471/ab2c86>
- [43] N.-N. Ma, T.-L. Zhao, W.-X. Wang, and H.-F. Zhang, *Phys. Rev. C* 107 (2023) 014310. <https://link.aps.org/doi/10.1103/PhysRevC.107.014310>
- [44] Z. Jin, M. Yan, H. Zhou, A. Cheng, Z. Ren, and J. Liu, *Phys. Rev. C* 108 (2023) 014326. <https://link.aps.org/doi/10.1103/PhysRevC.108.014326>
- [45] H.-Q. You, R.-H. Wu, H.-Z. Su, J.-J. Li, H.-Q. Zhang, and X.-T. He, *Phys. Rev. C* 110 (2024) 024319. <https://link.aps.org/doi/10.1103/PhysRevC.110.024319>
- [46] J. He, W.-B. He, Y.-G. Ma, and S. Zhang, *Phys. Rev. C* 104 (2021) 044902. <https://link.aps.org/doi/10.1103/PhysRevC.104.044902>
- [47] Z. M. Niu, H. Z. Liang, B. H. Sun, W. H. Long, and Y. F. Niu, *Phys. Rev. C* 99 (2019) 064307. <https://link.aps.org/doi/10.1103/PhysRevC.99.064307>
- [48] F. Minato, Z. Niu, and H. Liang, *Phys. Rev. C* 106 (2022) 024306. <https://link.aps.org/doi/10.1103/PhysRevC.106.024306>
- [49] C. Ma, Y. Lu, Y. Lei, and Y. M. Zhao, *Phys. Rev. C* 107 (2023) 034316. <https://link.aps.org/doi/10.1103/PhysRevC.107.034316>
- [50] M. Agostini, G. Benato, and J. A. Detwiler, *Phys. Rev. D* 96 (2017) 053001. <https://link.aps.org/doi/10.1103/PhysRevD.96.053001>
- [51] F. F. Deppisch and G. Van Gofrier, *Phys. Rev. D* 104 (2021) 055040. <https://link.aps.org/doi/10.1103/PhysRevD.104.055040>
- [52] J. Ebert, M. Fritts, D. Gehre, C. Göbbling, C. Hagner, N. Heidrich, et al. (The COBRA Collaboration), *Phys. Rev. C* 94 (2016) 024603. <https://link.aps.org/doi/10.1103/PhysRevC.94.024603>
- [53] B. Lehnert, M. Hult, G. Lutter, G. Marissens, S. Oberstedt, H. Stroh, et al., *Phys. Rev. C* 105 (2022) 045801. <https://link.aps.org/doi/10.1103/PhysRevC.105.045801>
- [54] N. Schunck, K. R. Quinlan, and J. Bernstein, *J Phys. G* 47 (2020) 104002. <https://dx.doi.org/10.1088/1361-6471/aba4fa>
- [55] X. Wang, L. Zhu, and J. Su, *Phys. Rev. C* 104 (2021) 034317. <https://link.aps.org/doi/10.1103/PhysRevC.104.034317>
- [56] Y. Wang, X. Zhang, Z. Niu, and Z. Li, *Phys. Lett. B* 830 (2022) 137154. <https://doi.org/10.1016/j.physletb.2022.137154>
- [57] L. Neufcourt, Y. Cao, S. A. Giuliani, W. Nazarewicz, E. Olsen, and O. B. Tarasov, *Phys. Rev. C* 101 (2020) 044307.

- <https://link.aps.org/doi/10.1103/PhysRevC.101.044307>
- [58] L. Neufcourt, Y. Cao, W. Nazarewicz, E. Olsen, and F. Viens, Phys. Rev. Lett. 122 (2019) 062502. <https://link.aps.org/doi/10.1103/PhysRevLett.122.062502>
- [59] M. Salinas and J. Piekarewicz, Phys. Rev. C 107 (2023) 045802. <https://link.aps.org/doi/10.1103/PhysRevC.107.045802>
- [60] Z. Zhang and L.-W. Chen, Phys. Rev. C 108 (2023) 024317. <https://link.aps.org/doi/10.1103/PhysRevC.108.024317>
- [61] Y.-L. Cheng, S. Shi, Y.-G. Ma, H. Stöcker, and K. Zhou, Phys. Rev. C 107 (2023) 064909. <https://link.aps.org/doi/10.1103/PhysRevC.107.064909>
- [62] C.-W. Ma, X.-X. Chen, X.-B. Wei, D. Peng, H.-L. Wei, Y.-T. Wang, et al., Phys. Rev. C 108 (2023) 044606. <https://link.aps.org/doi/10.1103/PhysRevC.108.044606>
- [63] Y.-H. Dang, J.-S. Li, and D.-H. Zhang, Chin. Phys. C 48 (2024) 1. <http://hepnp.ihep.ac.cn/en/article/id/1fb335f6-421a-47df-8f1c-5f2d99b43b1b>
- [64] R. Utama, W.-C. Chen, and J. Piekarewicz, J Phys. G 43 (2016) 114002. <https://dx.doi.org/10.1088/0954-3899/43/11/114002>
- [65] Y. Ma, C. Su, J. Liu, Z. Ren, C. Xu, and Y. Gao, Phys. Rev. C 101 (2020) 014304. <https://link.aps.org/doi/10.1103/PhysRevC.101.014304>
- [66] D. Wu, C. L. Bai, H. Sagawa, and H. Q. Zhang, Phys. Rev. C 102 (2020) 054323. <https://link.aps.org/doi/10.1103/PhysRevC.102.054323>
- [67] X.-X. Dong, R. An, J.-X. Lu, and L.-S. Geng, Phys. Rev. C 105 (2022) 014308. <https://link.aps.org/doi/10.1103/PhysRevC.105.014308>
- [68] X.-X. Dong, R. An, J.-X. Lu, and L.-S. Geng, Phys. Lett. B 838 (2023) 137726. <https://doi.org/10.1016/j.physletb.2023.137726>
- [69] J. Xu and P. Papakonstantinou, Phys. Rev. C 105 (2022) 044305. <https://link.aps.org/doi/10.1103/PhysRevC.105.044305>
- [70] S. Wesolowski, N. Klco, R. J. Furnstahl, D. R. Phillips, and A. Thapaliya, J Phys. G 43 (2016) 074001. <https://dx.doi.org/10.1088/0954-3899/43/7/074001>
- [71] J. Margueron, R. Hoffmann Casali, and F. Gulminelli, Phys. Rev. C 97 (2018) 025805. <https://link.aps.org/doi/10.1103/PhysRevC.97.025805>
- [72] L. Yang, C. Lin, Y. Zhang, P. Wen, H. Jia, D. Wang, et al., Phys. Lett. B 807 (2020) 135540. <https://doi.org/10.1016/j.physletb.2020.135540>
- [73] Y. Lim and J. W. Holt, Phys. Rev. C 103 (2021) 025807. <https://link.aps.org/doi/10.1103/PhysRevC.103.025807>
- [74] J. Xu, J. Zhou, Z. Zhang, W.-J. Xie, and B.-A. Li, Phys. Lett. B 810 (2020) 135820. <https://doi.org/10.1016/j.physletb.2020.135820>
- [75] A. Maselli, A. Sabatucci, and O. Benhar, Phys. Rev. C 103 (2021) 065804. <https://link.aps.org/doi/10.1103/PhysRevC.103.065804>
- [76] I. Svensson, A. Ekström, and C. Forssén, Phys. Rev. C 105 (2022) 014004. <https://link.aps.org/doi/10.1103/PhysRevC.105.014004>
- [77] D. Chatterjee, F. Gulminelli, A. R. Raduta, and J. Margueron, Phys. Rev. C 96 (2017) 065805. <https://link.aps.org/doi/10.1103/PhysRevC.96.065805>
- [78] C. Drischler, R. J. Furnstahl, J. A. Melendez, and D. R. Phillips, Phys. Rev. Lett. 125 (2020) 202702. <https://link.aps.org/doi/10.1103/PhysRevLett.125.202702>
- [79] W. G. Newton and G. Crocombe, Phys. Rev. C 103 (2021) 064323. <https://link.aps.org/doi/10.1103/PhysRevC.103.064323>
- [80] D. A. Godzieba, R. Gamba, D. Radice, and S. Bernuzzi, Phys. Rev. D 103 (2021) 063036. <https://link.aps.org/doi/10.1103/PhysRevD.103.063036>
- [81] W.-J. Xie and B.-A. Li, J Phys. G 48 (2021) 025110. <https://dx.doi.org/10.1088/1361-6471/abd25a>
- [82] S. M. A. Imam, N. K. Patra, C. Mondal, T. Malik, and B. K. Agrawal, Phys. Rev. C 105 (2022) 015806. <https://link.aps.org/doi/10.1103/PhysRevC.105.015806>
- [83] G. Grams, R. Somasundaram, J. Margueron, and E. Khan, Phys. Rev. C 106 (2022) 044305. <https://link.aps.org/doi/10.1103/PhysRevC.106.044305>
- [84] N. K. Patra, S. M. A. Imam, B. K. Agrawal, A. Mukherjee, and T. Malik, Phys. Rev. D 106 (2022) 043024. <https://link.aps.org/doi/10.1103/PhysRevD.106.043024>
- [85] L.-G. Pang and X.-N. Wang, Nucl. Sci. Tech. 34 (2023) 194. <https://doi.org/10.1007/s41365-023-01345-6>
- [86] M. V. Beznogov and A. R. Raduta, Phys. Rev. C 107 (2023) 045803. <https://link.aps.org/doi/10.1103/PhysRevC.107.045803>

- [87] D. Oliinychenko, A. Sorensen, V. Koch, and L. McLerran, *Phys. Rev. C* 108 (2023) 034908. <https://link.aps.org/doi/10.1103/PhysRevC.108.034908>
- [88] M. Qiu, B.-J. Cai, L.-W. Chen, C.-X. Yuan, and Z. Zhang, *Phys. Lett. B* 849 (2024) 138435. <https://doi.org/10.1016/j.physletb.2023.138435>
- [89] A. R. Raduta, M. V. Beznogov, and M. Oertel, *Phys. Lett. B* 853 (2024) 138696. <https://doi.org/10.1016/j.physletb.2024.138696>
- [90] J. Zhou, J. Xu, and P. Papakonstantinou, *Phys. Rev. C* 107 (2023) 055803. <https://link.aps.org/doi/10.1103/PhysRevC.107.055803>
- [91] M. V. Beznogov and A. R. Raduta, *Phys. Rev. C* 110 (2024) 035805. <https://link.aps.org/doi/10.1103/PhysRevC.110.035805>
- [92] V. Carvalho, M. Ferreira, and C. Providencia, *Phys. Rev. D* 109 (2024) 123038. <https://link.aps.org/doi/10.1103/PhysRevD.109.123038>
- [93] D. Higdon, J. D. McDonnell, N. Schunck, J. Sarich, and S. M. Wild, *J Phys. G* 42 (2015) 034009. <https://dx.doi.org/10.1088/0954-3899/42/3/034009>
- [94] J. A. Melendez, S. Wesolowski, and R. J. Furnstahl, *Phys. Rev. C* 96 (2017) 024003. <https://link.aps.org/doi/10.1103/PhysRevC.96.024003>
- [95] B. Cauchois, H. Lü, D. Boilley, and G. Royer, *Phys. Rev. C* 98 (2018) 024305. <https://link.aps.org/doi/10.1103/PhysRevC.98.024305>
- [96] G. F. Bertsch and D. Bingham, *Phys. Rev. Lett.* 119 (2017) 252501. <https://link.aps.org/doi/10.1103/PhysRevLett.119.252501>
- [97] J. Hu, P. Wei, and Y. Zhang, *Phys. Lett. B* 798 (2019) 134982. <https://doi.org/10.1016/j.physletb.2019.134982>
- [98] T. M. Sprouse, R. Navarro Perez, R. Surman, M. R. Mumpower, G. C. McLaughlin, and N. Schunck, *Phys. Rev. C* 101 (2020) 055803. <https://link.aps.org/doi/10.1103/PhysRevC.101.055803>
- [99] K. Kravvaris, K. R. Quinlan, S. Quaglioni, K. A. Wendt, and P. Navrátil, *Phys. Rev. C* 102 (2020) 024616. <https://link.aps.org/doi/10.1103/PhysRevC.102.024616>
- [100] C. Drischler, J. A. Melendez, R. J. Furnstahl, and D. R. Phillips, *Phys. Rev. C* 102 (2020) 054315. <https://link.aps.org/doi/10.1103/PhysRevC.102.054315>
- [101] A. E. Lovell, A. T. Mohan, and P. Talou, *J Phys. G* 47 (2020) 114001. <https://dx.doi.org/10.1088/1361-6471/ab9f58>
- [102] J. Xu, Z. Zhang, and B.-A. Li, *Phys. Rev. C* 104 (2021) 054324. <https://link.aps.org/doi/10.1103/PhysRevC.104.054324>
- [103] O. Sürer, F. M. Nunes, M. Plumlee, and S. M. Wild, *Phys. Rev. C* 106 (2022) 024607. <https://link.aps.org/doi/10.1103/PhysRevC.106.024607>
- [104] D. Gazda, T. Yadanar Htun, and C. Forssén, *Phys. Rev. C* 106 (2022) 054001. <https://link.aps.org/doi/10.1103/PhysRevC.106.054001>
- [105] M. Imbrišak and K. Nomura, *Phys. Rev. C* 108 (2023) 024321. <https://link.aps.org/doi/10.1103/PhysRevC.108.024321>
- [106] Y. Saito, I. Dillmann, R. Krücken, M. R. Mumpower, and R. Surman, *Phys. Rev. C* 109 (2024) 054301. <https://link.aps.org/doi/10.1103/PhysRevC.109.054301>
- [107] X.-Y. Wang, Y. Cui, Y. Tian, K. Zhao, and Y.-X. Zhang, *Chin. Phys. C* 48 (2024) 084105. <http://hepnp.ihep.ac.cn/en/article/doi/10.1088/1674-1137/ad47a7>
- [108] A. E. Barzakh, D. V. Fedorov, V. S. Ivanov, P. L. Molkanov, F. V. Moroz, S. Y. Orlov, et al., *Phys. Rev. C* 95 (2017) 044324. <https://link.aps.org/doi/10.1103/PhysRevC.95.044324>
- [109] M. Anselment, W. Faubel, S. Göring, A. Hanser, G. Meisel, H. Rebel, and G. Schatz, *Nucl. Phys. A* 451 (1986) 471. [https://doi.org/10.1016/0375-9474\(86\)90071-0](https://doi.org/10.1016/0375-9474(86)90071-0)
- [110] S. Péru, S. Hilaire, S. Goriely, and M. Martini, *Phys. Rev. C* 104 (2021) 024328. <https://link.aps.org/doi/10.1103/PhysRevC.104.024328>
- [111] T. Day Goodacre, A. V. Afanasjev, A. E. Barzakh, B. A. Marsh, S. Sels, P. Ring, et al., *Phys. Rev. Lett.* 126 (2021) 032502. <https://link.aps.org/doi/10.1103/PhysRevLett.126.032502>
- [112] S. Akkoyun, T. Bayram, S. O. Kara, and A. Sinan, *J Phys. G* 40 (2013) 055106. <https://dx.doi.org/10.1088/0954-3899/40/5/055106>
- [113] Z.-X. Yang, X.-H. Fan, T. Naito, Z.-M. Niu, Z.-P. Li, and H. Liang, *Phys. Rev. C* 108 (2023) 034315. <https://link.aps.org/doi/10.1103/PhysRevC.108.034315>

- [114] X. Zhang, X. Liu, H. Zheng, W. Lin, R. Wada, J. Han, et al., *IEEE Transactions on Nuclear Science*, 1 (2024). [10.1109/TNS.2024.3451400](https://doi.org/10.1109/TNS.2024.3451400)
- [115] R. F. Casten, D. S. Brenner, and P. E. Haustein, *Phys. Rev. Lett.* 58 (1987) 658. <https://link.aps.org/doi/10.1103/PhysRevLett.58.658>
- [116] I. Angeli, *J Phys. G* 17 (1991) 439. <https://dx.doi.org/10.1088/0954-3899/17/4/006>
- [117] R. F. Casten and N. V. Zamfir, *J Phys. G* 22 (1996) 1521. <https://dx.doi.org/10.1088/0954-3899/22/11/002>
- [118] Z. Sheng, G. Fan, J. Qian, and J. Hu, *Eur. Phys. J. A* 51 (2015) 40. <https://doi.org/10.1140/epja/i2015-15040-1>
- [119] N. Srivastava, G. Hinton, A. Krizhevsky, I. Sutskever, and R. Salakhutdinov, *J Mach. Learn. Res.* 15 (2014) 1929. <http://jmlr.org/papers/v15/srivastava14a.html>
- [120] Y. Gal, *Uncertainty in Deep Learning* (University of Cambridge, Cambridge, 2016).
- [121] R. Zhang, M. E. Merkel, S. Beck, and C. Ederer, *Phys. Rev. Res.* 4, 043082 (2022). <https://link.aps.org/doi/10.1103/PhysRevResearch.4.043082>
- [122] D. Y. Huo, Z. Wei, K. Wu, C. Han, Y. X. Wang, Y. N. Han, et al., *Eur. Phys. J. A* 59 (2023) 265. <https://doi.org/10.1140/epja/s10050-023-01189-z>
- [123] B. E. Kowal, K. M. Graczyk, A. M. Ankowski, R. D. Banerjee, H. Prasad, and J. T. Sobczyk, *Phys. Rev. C* 110 (2024) 025501. <https://link.aps.org/doi/10.1103/PhysRevC.110.025501>
- [124] M. J. Wen and E. B. Tadmor, *npj Comput. Mater.* 6 (2020) 124. <https://doi.org/10.1038/s41524-020-00390-8>
- [125] E. Hüllermeier and W. Waegeman, *Mach. Learn.* 110 (2021) 457. <https://doi.org/10.1007/s10994-021-05946-3>
- [126] I. Angeli and K. Marinova, *At. Data Nucl. Data Tables* 99 (2013) 69. <https://doi.org/10.1016/j.adt.2011.12.006>
- [127] T. Li, Y. Luo, and N. Wang, *At. Data Nucl. Data Tables* 140 (2021) 101440. <https://doi.org/10.1016/j.adt.2021.101440>
- [128] P. Möller and A. J. Sierk and T. Ichikawa and H. Sagawa, *At. Data Nucl. Data Tables* 109-110 (2012) 1. <https://doi.org/10.1016/j.adt.2015.10.002>
- [129] B. Nerlo-Pomorska and K. Pomorski, *Z. Phys. A* 348 (1994) 169, arXiv:nucl-th/9401015. [10.1007/BF01291913](https://doi.org/10.1007/BF01291913)
- [130] T. Bayram, S. Akkoyun, S. O. Kara, and A. Sinan, *Acta Phys. Polon. B* 44 (2013) 1791. [10.5506/APhysPolB.44.1791](https://doi.org/10.5506/APhysPolB.44.1791)
- [131] G. D. Alkhazov, A. E. Barzakh, V. A. Bolshakov, V. P. Denisov, V. S. Ivanov, Y. Y. Sergeev, et al., *Z Phys. A* 337 (1990) 257. <https://doi.org/10.1007/BF01289691>
- [132] A. E. Barzakh, J. G. Cubiss, A. N. Andreyev, M. D. Seliverstov, B. Andel, S. Antalic, et al., *Phys. Rev. C* 99 (2019) 054317. <https://link.aps.org/doi/10.1103/PhysRevC.99.054317>
- [133] S. Malbrunot-Ettenauer, S. Kaufmann, S. Bacca, C. Barbieri, J. Billowes, M. L. Bissell, et al., *Phys. Rev. Lett.* 128 (2022) 022502. <https://link.aps.org/doi/10.1103/PhysRevLett.128.022502>
- [134] F. Sommer, K. König, D. M. Rossi, N. Everett, D. Garand, R. P. de Groote, et al., *Phys. Rev. Lett.* 129 (2022) 132501. <https://link.aps.org/doi/10.1103/PhysRevLett.129.132501>
- [135] K. König, S. Fritzsche, G. Hagen, J. D. Holt, A. Klose, J. Lantis, et al., *Phys. Rev. Lett.* 131 (2023) 102501. <https://link.aps.org/doi/10.1103/PhysRevLett.131.102501>
- [136] M. M. Sharma, G. Lalazissis, J. König, and P. Ring, *Phys. Rev. Lett.* 74 (1995) 3744. <https://link.aps.org/doi/10.1103/PhysRevLett.74.3744>
- [137] G. A. Lalazissis and S. E. Massen, *Phys. Rev. C* 53 (1996) 1599. <https://link.aps.org/doi/10.1103/PhysRevC.53.1599>
- [138] G. Miller, A. Beck, S. May-Tal Beck, L. Weinstein, E. Piasetzky, and O. Hen, *Phys. Lett. B* 793 (2019) 360. <https://doi.org/10.1016/j.physletb.2019.05.010>
- [139] W. Cosyn and J. Ryckebusch, *Phys. Lett. B* 820 (2021) 136526. <https://doi.org/10.1016/j.physletb.2021.136526>